Incorporation of Thermal Rotation of Drifting Ions into Mobility Calculations: Drastic Effect for Heavier Buffer Gases

Alexandre A. Shvartsburg,[†] Stefan V. Mashkevich,[‡] and K. W. Michael Siu*,[†]

Department of Chemistry and Center for Research in Mass Spectrometry, York University, 4700 Keele Street, Toronto, Ontario, Canada M3J 1P3, and Merrill Lynch Global Headquarters, World Financial Center, North Tower, 250 Vesey Street, New York, New York 10281

Received: May 11, 2000; In Final Form: August 17, 2000

Ion mobility spectrometry (IMS) assumes increasing prominence among the tools for characterization of gas-phase ions and analysis of complex mixtures. The assignment of features observed in IMS experiments to specific structures necessitates the calculation of mobilities for plausible candidate geometries. All previous methods for these calculations have assumed that the ion−buffer gas collisions are fully elastic and that the drifting ions cannot rotate during a collisional event. This paradigm does not mesh well with the fact that the measured quantity is the orientationally averaged collision integral. Here we model the effect of the thermal rotation of drifting ions on their mobility. Simulations show that the cross sections for rotating objects are greater than those for static ones because a molecular image "blurs out" over the duration of collision. This increase is particularly significant for light and elongated ions. For a given ion, the effect is dramatically larger in heavy buffer gases, in some cases exceeding 20%. Present findings reveal the importance of accounting for the nonelasticity of scattering in ion mobility calculations.

I. Introduction into Ion Mobility Calculations

A decade ago, Hill and co-workers[1] had opined that "although ion mobility spectrometry (IMS) is considered an old technology, in many ways it is a new technology waiting to be rediscovered". This prediction has been fulfilled amply during the 1990s. The first major experimental development was the combination of IMS with mass spectrometry by Bowers and co-workers.[2] Their tandem quadrupole drift tube apparatus enabled a breakthrough in the structural characterization of gas-phase cluster ions, in particular carbon species.[3] Shortly thereafter, Jarrold and Constant[4] invented the annealing technique that permits the determination of isomerization energies and pathways by monitoring the dependence of measured mobilities on the kinetic energy of ions injected into a drift tube. The utility of IMS/MS as a structural probe was broadened greatly by its coupling with MALDI and electrospray sources,[5,6] with which conformational analysis of biological molecules became possible. Concurrently, the resolution of IMS was improved by an order of magnitude through the use of higher drift fields and longer tubes.[7−9] The development of high-field asymmetric waveform ion mobility spectrometry (FAIMS)[10,11] has enabled one to readily measure mobilities at high drift fields, thus permitting the separation of species based on their mobility as a function of field intensity. Most recently, Clemmer and collaborators[12−14] have equipped an IMS/MS instrument with an ion trap and replaced the quadrupole mass spectrometer by time-of-flight mass selection. These two innovations have drastically augmented the efficiency and sensitivity of IMS/MS in analytical applications by attaining a near-complete utilization of the original ion signal.

As long as IMS had been used as only an analytical tool, one could assign the features observed in the drift time distributions (the ion mobility spectra) simply by matching them with those measured for candidate analytes. To characterize a species of unknown structure, one has to compare the measured mobility with values calculated for a number of plausible candidate geometries. This has provided a major impetus for the development of theoretical techniques to compute the mobility for an arbitrary ion. Ion mobility measurements are usually performed in the low-field limit, where mobility is independent of the field intensity. In this limit, the evaluation of ionic mobilities is reduced to the calculation of a series of orientationally averaged collision integrals.[15] When the buffer gas atoms are much lighter than the drifting ions (Rayleigh limit), the above series may be truncated at its first term—the first-order collision integral (cross section) $\Omega_{avg}^{(1,1)}$—to produce the well-known expression

$$K = \frac{(18\pi)^{1/2}}{16}\left[\frac{1}{m}+\frac{1}{m_B}\right]^{1/2}\frac{ze}{(k_BT)^{1/2}}\frac{1}{\Omega_{avg}^{(1,1)}}\frac{1}{N} \qquad (1)$$

Here K is the mobility, m and ze are the ionic mass and charge, respectively, m_B and N are the mass and number density of buffer gas atoms, and T is the gas temperature. The first method for mobility calculations (known as the "projection approximation") has simply equated the cross sections to orientationally averaged projections. This method, dating back[16] to 1925, has been the only one available[3] for analysis of ion mobility data until a few years ago. The advent of high-resolution mobility measurements[7] has substantially tightened the tolerable error margin of calculations necessary for confident structural assignments of observed features. This has prompted a rapid development of increasingly more sophisticated techniques for mobility calculations: (I) the exact hard-spheres scattering (EHSS) model,[17] where the cross section is evaluated rigorously under the assumption of pairwise hard-sphere potentials between a buffer gas atom and each atom in the ion, (II) the trajectory

* To whom correspondence should be addressed.
[†] York University.
[‡] Merrill Lynch Global Headquarters.

10.1021/jp001753a CCC: $19.00
Published on Web 09/29/2000

method in which the collision integral is calculated accounting for a realistic interaction potential between the ion and buffer gas atoms,[18,19] and (III) the scattering on electron density isosurfaces (SEDI) treatment,[20] where an ion is represented via its electronic cloud rather than nuclear coordinates, which emulates more closely the physical reality of molecular scattering and allows one to simulate the dependence of mobility on ionic charge. Most recently, the advantages of SEDI and trajectory calculations have been combined in the hybrid SEDI-TC formalism.[21] These methods have greatly increased the accuracy of mobility calculations, which in many instances has proven critical for correct structural analysis of experimental data.[18−24] With further augmentation of available computing power, the above progression of improvements could be taken to its ultimate limit—evaluation of mobilities by propagation of classical molecular dynamics trajectories in the ion−buffer gas interaction potential defined from the first principles.

II. Incorporation of Rotational Degrees of Freedom in Mobility Calculations

All mobility calculation methods designed so far have assumed fully elastic collisions. In reality, the inelasticity of scattering arises from the transfer of energy between translational motion of colliding species and the vibrational or rotational degrees of freedom of the ion. Unlike the coupling between translation and vibration, the coupling between translation and rotation can be modeled without delving into the internal properties of an ion. The existence of rotational degrees of freedom influences ionic mobilities in two ways. First, ions drifting in a gas are subject to thermal rotation, and this rotation prior to a collision with a buffer gas atom may affect the probability and location of impact. The fact that all known methods for mobility calculations evaluate the orientationally averaged collision integral indeed implies the existence of thermal rotation. However, these methods have essentially assumed that thermal rotation occurs between, but not during, collisions with buffer gas atoms. This is equivalent to the "rotational sudden approximation" well-known in scattering theory. Second, the velocity and the scattering angle of an atom bouncing off a target depend on whether its spatial orientation is fixed or free (irrespective of whether it has actually been rotating prior to collision). In principle, both effects can be completely described (within the rigid rotor approximation) by requiring the conservation of angular momentum and total kinetic energy. Here we advance toward that goal by modeling the first (kinematic) effect. This evidently amounts to the incorporation of molecular rotation into the projection approximation that can formally be set as

$$\Omega = \frac{1}{4\pi}\int_0^{2\pi} \mathrm{d}\theta \int_0^{\pi} \mathrm{d}\varphi \sin\varphi \int_0^{2\pi} \mathrm{d}\gamma \int_0^{\infty} b\, \mathrm{d}b\, M(\theta,\varphi,\gamma,b) \quad (2)$$

where M is an integer-valued function that is unity when a hard-sphere collision occurs for a geometry defined by θ, φ, γ, b and null otherwise. (The difference from earlier work is that θ, φ, and γ are now time-dependent.) Although eq 2 is known to yield inaccurate absolute collision integrals for a number of systems,[18−24] its use should allow an estimation of the possible relative impact of ionic rotation on mobilities.

The computational implementation is as follows. The tensor of inertia of an ion is calculated and diagonalized to determine the three principal axes of rotation and the corresponding momenta of inertia (I_i). The rotation is then modeled using the dynamic Euler equations (the differential equations for the projections of angular velocity on the principal axes). The initial values for these projections are simulated using the Metropolis Monte Carlo algorithm such that the kinetic energy of rotation around each axis conforms to the Gibbs distribution. That is, the probability distribution for each component of angular velocity w_i is

$$P(w_i) = \exp(-I_i w_i^2/(2k_B T)) \quad (3)$$

By assumption of thermal equilibration, the rotational temperature of the ion equals the temperature of the buffer gas. The initial spatial orientation of the ion is, of course, random. Substituting the initial conditions for atomic coordinates and angular velocities into the analytical solutions of the Euler equations yields the time dependence of the projections. This is transformed into the time dependence of Euler angles, from which the coordinates of atoms making up the ion are derived numerically as a function of time. The rest of the code resembles the setup of the projection approximation.[3] A buffer gas atom is propagated starting from a distance large enough to avoid touching the ion regardless of its orientation, and the linear trajectory is followed to find out whether a collision with the ion occurs. To evaluate the projection, the probability of collision is integrated over the impact parameter and Maxwell distribution of relative translational velocities, g, between an ion and a buffer gas atom:

$$P(g) = g^2 \exp(-\mu g^2/(2k_B T)) \quad (4)$$

where μ is the reduced mass of the system, $\mu = mm_B/(m + m_B)$. As appropriate for any Monte Carlo approach, the statistical error of the present model is inversely proportional to the square root of the number of sampled trajectories. Millions of trajectories have to be averaged in order to achieve a reasonable convergence of calculated mobilities.

The model described above rigorously incorporates the precession of an instantaneous axis of rotation (that is, the temporal drift of angular velocity direction) that happens whenever the initial angular velocity is not aligned with a principal axis of inertia. In practice, that precession is much slower than the rotation itself; consequently, the effect of rotation on ionic mobility should only be altered in a minor way. To verify this, we have set up a simplified treatment where the precession is ignored, and thus the angular velocity is constant throughout the simulation. (Its projections on the principal axes, however, change because those axes rotate together with the molecule in the laboratory frame of reference.) This approximate model has been tested for a number of systems, including monocyclic carbon rings with 8−16 atoms and several three-dimensional organic molecules such as pentamine and diaminobutane. In all cases, the results are indistinguishable from those produced by the exact solution. As this model neglecting precession bypasses the time-consuming integration of equations of motion, the computational expense is reduced by orders of magnitude. Most data reported below have been obtained via this shortcut. (When one momentum of inertia for a molecule is null, there is no precession. So, the approximate model is rigorous for linear species, including the pure and hydrogenated carbon chains considered below.)

III. Results

Before proceeding to specific examples of the effect of thermal rotation on ionic mobilities, it is worthwhile to assess several qualitative trends. First, calculated cross sections always

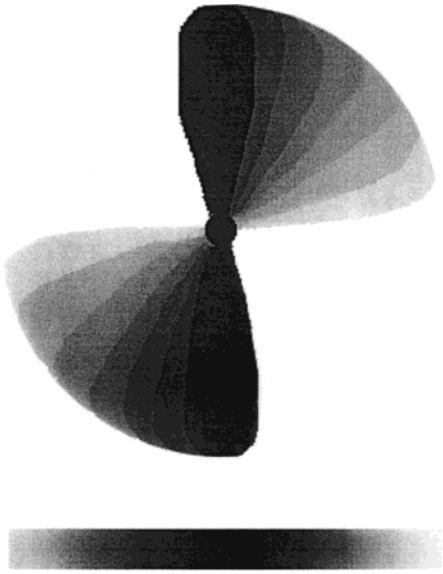

Figure 1. Diagram illustrating how the projections of an aircraft propeller on two perpendicular planes increase when the propeller rotates. The shadow of the static propeller is black, while that of the blurred-out rotating propeller is in gray scale.

increase after rotation is incorporated. This can be rationalized readily by considering an aircraft propeller (Figure 1). When it rotates, its projection increases along each of the three directions shown (in fact, along any arbitrary direction). Hence its orientationally averaged projection must also increase. In a chemical context, a propeller is a model for a highly elongated molecule. This simple "blurring vision" phenomenon applies to all nonspherical geometries (obviously the projection of a perfect sphere is not affected by its rotation). Second, it immediately follows from here that, other factors being equal, the increase in projection due to rotation should be larger for more elongated objects. Third, the distribution of the angular velocities of molecular rotation and the distribution of the relative velocities of the ion and the buffer gas atoms both scale as a square root of temperature. As the problem is invariant with respect to the scaling of all velocities by a constant factor, the effect of thermal rotation on ionic mobilities would not have depended on the buffer gas temperature. However, the cross sections of irrotational ions increase upon cooling as the effective collision radii between atoms in the ion and buffer gas become larger.[25] This reduces the aspect ratio for any geometry; thus, the influence of thermal rotation on ionic mobility should slightly decrease at lower temperatures. Fourth, the effect has to be stronger for heavier buffer gases. Indeed, the mean relative velocity of an ion and a buffer gas atom is inversely proportional to the square root of their reduced mass. As a result, this velocity decreases with the increasing mass of the buffer gas atom, and the whole distribution of velocities shifts accordingly. The distribution of the angular velocities of a rotating molecule obviously does not depend on the identity of the buffer gas atom. Hence, ionic rotation is relatively faster in heavier gases, and the effect of rotation has to be larger.

For a systematic quantitative investigation, we have chosen the example of carbon clusters. These species assume a great variety of morphologies, undergoing transitions from straight chains to monocyclic and bicyclic rings to graphite sheets to fullerenes and their oligomers as the number of atoms increases. This unique structural diversity, an extensive set of available experimental data (including as a function of buffer gas temperature), and a very accurate knowledge of carbon cluster geometries in theory have made this system a customary testing

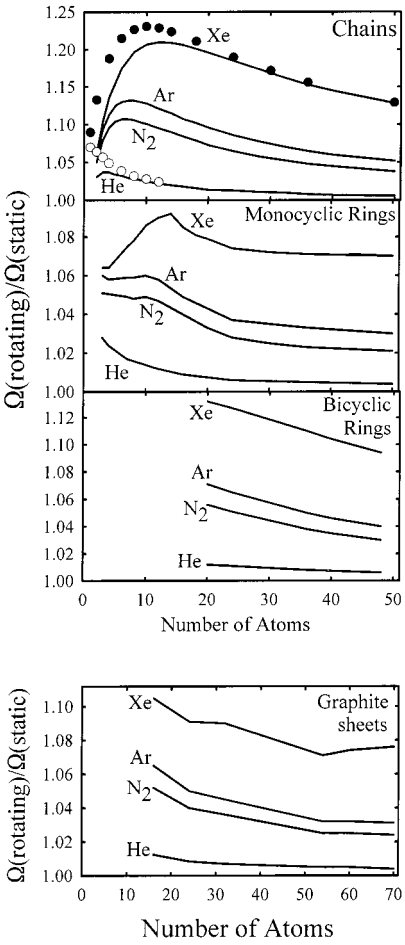

Figure 2. Relative increases of orientationally averaged projections for carbon cluster ions belonging to various isomeric families due to molecular thermal rotation (solid lines). We have assumed the collision distances of 2.75 Å for C−He, 3.15 Å for C−Ar, 3.75 Å for C− N_2, and 3.55 Å for C−Xe; however, the results are insensitive to the choice of these values within reason. Cluster geometries were identical to those adopted in previous calculations[17,19,21] of mobilities for C_n ions. The following are displayed in order, starting at the top: cumulenic linear chains and rotationally symmetric monocyclic rings with C−C bond lengths of 1.29 Å, MNDO-optimized bicyclic rings, and graphite sheets. Empty and filled circles are for the hydrogen-terminated carbon chains in He and Xe (we have assumed $R_{H-He} = 2.2$ Å and $R_{H-Xe} = 3.0$ Å, but the findings are again insensitive to a reasonable variation in these values).

ground for new methods in mobility calculations.[17−19,21,23] The effect of thermal rotation on the orientationally averaged projections of various C_n ions is demonstrated in Figure 2. This effect is expressed in terms of Ω_r/Ω_s, where Ω_r and Ω_s are orientationally averaged projections for rotating and static ions, respectively. We have considered four commonly used buffer gases: helium, nitrogen, argon, and xenon. The results plotted in Figure 2 are in complete accordance with the qualitative trends outlined above. Thermal rotation always increases the projections, more so for heavier buffer gases regardless of the cluster size or shape. The enhancement of the effect by massive gas atoms is drastic, often by a factor of 10−20 or more from He to Xe.[26] With any buffer gas, the largest increases occur for linear chains, which is not surprising considering that their aspect ratios are higher than those of any other geometry conceivable. The effect for bicyclic rings exceeds that for monocyclic ones with the same *n*; the former are elongated along all three principal axes while the latter are elongated along two only (the rotation about the axis orthogonal to the ring plane does not affect the cross section). Interestingly, the relative increase of

projection due to thermal rotation generally maximizes at a certain cluster size. This happens because very small ions are inherently not elongated significantly, irrespective of the shape, and the effect of rotation is necessarily modest even though the rotation is fast. At the other extreme, very large molecules have high momenta of inertia and rotate slowly; therefore, the effect is small even if the aspect ratio is high. (The effect is obviously null in the macroscopic limit.) Within any structural family, the Ω_r/Ω_s ratio maximizes at larger cluster sizes when the mass of the buffer gas atom increases. For example, the maximum for C_n chains occurs at $n = 4$, 7, 8, and 12 with He, N_2, Ar, and Xe, respectively. This happens because (i) the slower rotation of a larger object is less slow, comparatively, than the slower motion of heavier buffer gas atoms and (ii) heavier buffer gas atoms tend to have larger collision radii, which reduces the effective aspect ratio of the ion (considering the ion−atom complex). The situation for the other morphologies is similar, except that for less elongated geometries (such as monocyclic rings or graphite sheets), there may be no maximum at all, at least with light buffer gases.

With some experience, one can roughly predict the magnitude of the increase of the orientationally averaged projection for any geometry without having actually performed the calculation. For example, graphite sheets are, like monocyclic rings, planar and elongated with respect to the two axes in their plane only. Therefore, thermal rotation should affect the mobilities of these two isomer families similarly, and calculations show this to be true (Figure 2). On the other hand, the mobilities of near-spherical fullerenes should be virtually unaffected by rotation. This indeed is the case, as Ω_r/Ω_s calculated for C_{60} and other fullerenes is ∼1.002, even in Xe, and is indistinguishable from unity in lighter gases. (The marginal increase in the case of Xe is due to the dips on the cage surface creating minute deviations from a perfect sphere.) Quasiplanar morphologies predicted for boron cluster ions[27−29] resemble the single-layer C_n graphite sheets, and the atomic mass of boron (10.8 amu) is close to that of carbon (12.0 amu). Hence, the mobilities of boron clusters ought to be affected by thermal rotation analogously to those of graphite sheets. In fact, the values of Ω_r/Ω_s calculated for B_n geometries ($n = 4-36$) range from ∼1.02 to ∼1.005 in He and from ∼1.07 to ∼1.04 in Ar, in a close agreement with the graphite sheet data (Figure 2).

To gauge the sensitivity of the effect to buffer gas temperature, one may estimate the collision distances at several temperatures and execute the code with those values. The mobility of the C_7 chain cation measured in He over the 78−355 K range is fit by R_{C-He} decreasing from 3.19 to 2.42 Å. We have tested these limiting values and found but a very minor difference in the resulting Ω_r/Ω_s. This negligible temperature effect should be even smaller for other, less elongated ion geometries. Hence we conclude that the relative effect of molecular thermal rotation on mobility is virtually constant over a large temperature range. This has allowed us to perform all calculations using simply the atom−buffer gas collision distances appropriate for room temperature.

As shown in Figure 2, Ω_r/Ω_s reaches a staggering value of 1.21 in the case of Xe buffer gas but it may approach 1.04 even in He. A correction of this magnitude is quite significant considering that the resolution of the best IMS apparata is presently[7] under 1% and that the error margin customarily allowed[3,5,30] in structural assignment of data is 2%. It should be pointed out that the geometries exhibiting the greatest Ω_r/Ω_s values need not necessarily be pure carbon chains. For example, hydrogen-terminated chains[31] exhibit a somewhat stronger rotation effect. This is readily understood, as two light H atoms extend the chain length (and thus elongation) while hardly increasing the momenta of inertia. Specifically, Ω_r/Ω_s increases to 1.23 for H−C_{10}−H in Xe (Figure 2) and 1.07 for H−C−H in He. Conversely, the rotation effect for chains terminated by atoms heavier than C (such as chlorine[32]) would be smaller than that for pure C_n. This pattern is quite general and is not limited to chains. For example, Leone and coworkers[33,34] have studied the mobilities of small aromatic hydrocarbons, such as benzene and naphthalene, in several gases. The ratio of Ω_r to Ω_s calculated for benzene is 1.04 in He, 1.11 in Ar, and 1.14 in Xe, while the same quantity for the C_6 ring (Figure 2) is 1.02, 1.06, and 1.07, respectively. The situation for bicyclic rings is similar; the increase of projection due to thermal rotation for a putative species consisting of two C_6 rings fused in plane ranges from 1% in He to 9% in Xe, while the effect computed for naphthalene is between 3% and 16%.

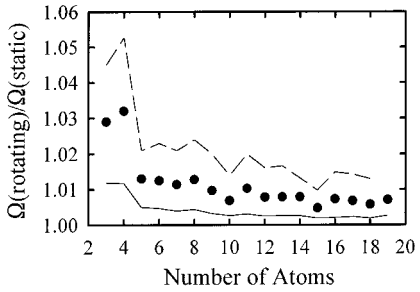

Figure 3. Relative increases of orientationally averaged projections for Si_n in He and Ar (solid and dashed lines, respectively) and Ge_n in Ar (circles) due to the thermal rotation of ions. Collision distances of 2.92 Å for Si−He and 3.32 Å for Si−Ar and Ge−Ar have been adopted. We have used the lowest-energy geometries found for Si_n cations.[20,22,35] For the sake of illustration, Ge and Si clusters have been assumed isomorphous, although in fact their geometries differ for some sizes in the $n > 13$ range slightly.[36]

The effect of rotation on cross sections for clusters of heavier atoms is generally less significant. For example, the mobilities of semiconductor cluster ions have recently been analyzed in detail to elucidate the growth habit of these species.[20,22,35−38] The Ω_r/Ω_s quantity for Si_n ions is lower than that for the carbon species of same nuclearity (Figure 3). This reflects not only a greater atom mass (28 versus 12 amu) but also much more compact packing of Si clusters. (A major drop in Ω_r/Ω_s at $n = 5$ is due to the transition from planar to less elongated three-dimensional structures.[20,22]) However, for some sizes the increase of the projection due to rotation is still over $\Omega_r/\Omega_s = 1.01$, even in the case of He buffer gas. For Ar, this increase is over 1.05. The effect for heavier group IV element clusters is naturally smaller but still is over 1.03 for Ge_n (Figure 3) and is ∼1.02 even for Pb_n (both in Ar). The above examples reveal that thermal rotation may materially influence mobilities not only for ions consisting of light atoms or for extremely elongated species but also for some reasonably compact ions as well.

In the last couple years, IMS techniques have been applied to the characterization of bio-organic ions and the analysis of complex biological mixtures.[6,8,13,14,39−44] A most relevant question is how the thermal rotation considered here impacts the mobilities of these relatively large species. It appears that the results for medium-sized and large proteins are not affected significantly, even for the fully unfolded conformations with high aspect ratios. That is, the increase of projection for protonated cytochrome *C* optimized for the +13, +15, +17, and +19 charge states[41] is not larger than $\Omega_r/\Omega_s = 1.005$ in the case of Ar buffer gas and is essentially nil in He. The rotation effect is, however, stronger for smaller biological ions such as

polypeptides and enzymatically cleaved peptides in protein digestion. For example, the projections for polyalanines in the $n = 10-20$ range[42] are elevated by about 1.005 in He, 1.02 in Ar, and 1.05−1.06 in Xe buffer gas. This effect is greater yet for smaller organic ions such as the aromatic hydrocarbons mentioned above. Similar values of Ω_r/Ω_s (1.07−1.11 in Ar buffer) are obtained for straight-chain saturated aliphatic hydrocarbons from ethane to *n*-tetradecane. For the more elongated acetylene and ethylene ions, the increase of projection in Ar reaches 1.13.

IV. Conclusions

We have made in ion mobility calculations the first step toward accounting for the inelastic nature of real ion−buffer gas collisions by considering the thermal rotation of drifting ions. An exact numerical treatment of this rotation reveals that the orientationally averaged projections of polyatomic ions always exceed the values computed for irrotational species using hitherto existing methods. This increase, due to the "blurring-out" of molecular images over the finite duration of collisions, is particularly substantial for objects with high aspect ratios and of modest size (because of their fast rotation). Since the projections of elongated species are affected disproportionately, the shift would not be systematic for all isomers observed in an arrival time distribution. Specifically, the separation between peaks would become larger. The magnitude of this effect for a given ion is greater with heavier buffer gas atoms, as their translational motion is slower and hence collisional events effectively last longer. For some elongated species, the increase of projection due to thermal rotation may reach 1.23 in Xe and 1.07 even in the He buffer. This increase may be greater yet for heavy polyatomic buffer gases occasionally used in mobility measurements, such as sulfur hexafluoride[45,46] (MW = 146 Da). Increases of this magnitude are highly significant considering that structural assignments made in much of the recent ion mobility work[18−24,35,36,47,48] critically hinge on calculations being accurate to within 1−2%. Of course, ion mobility experiments actually determine the orientationally averaged collision integrals that, in general, differ from the projections substantially. It is not presently clear whether the collision integrals would be affected by thermal rotation stronger or weaker than the projections. However, the effect is likely significant and the issue should be investigated further. Unfortunately, the interaction potentials of molecular ions with heavy buffer gas atoms have not been determined nearly as accurately as those with He.[18,19,22,36] This makes it difficult to compare our present results with the measurements, as the baseline cross sections without rotation could not be computed with the requisite accuracy.

In the meantime, our findings strongly suggest that the analysis of mobility measurements in heavy gases is subject to a larger degree of uncertainty. This observation compounds previously known problems associated with extracting structural assignments from mobilities in heavy gases. These problems include (i) high polarizability of heavy atoms, which induces strong long-range ion−buffer gas potentials, (ii) large van der Waals radii of heavy atoms, which decrease the difference in cross section between different ion isomers, (iii) smaller translational velocities of heavy atoms, which reduce the range of validity of the low drift field approximation (the governing criterion is that the ion drift velocity must be negligible compared to that of Brownian motion in the gas), and (iv) possible violation of the Rayleigh limit (that the mass of buffer gas atoms is infinitesimal compared to the masses of drifting ions), which necessitates complicated and tedious evaluations of higher-order collision integrals. For nonmonatomic buffers such as nitrogen, air, or SF_6, one additionally faces the issues of nonsphericity of the gas molecule and possible exchange of translational energy with its rotational and vibrational degrees of freedom. So, it is hardly surprising that virtually all structural assignments obtained so far using IMS have been derived from the data in He. Efforts to analyze the values measured in other gases have been mostly unsuccessful. For example, it has been noted[33] that the projection approximation produces reasonable values for mobilities of various ions measured in He but not for those measured in N_2. A growing understanding of the major difficulties involved in modeling the mobilities of polyatomic ions in heavy buffers increasingly favors He as a medium of choice, despite higher complexity and costs on the experimental side. On the other hand, attaining the highest possible experimental resolution may call for the use of heavier buffer gases, as they normally have higher thresholds for voltage breakdown. Creating the tools capable of analyzing such data remains a major theoretical challenge.

Acknowledgment. We thank Dr. Yi Mao and Professor Mark A. Ratner for providing us with their calculated structures for cytochrome *C* and various polypeptides and Dr. Charles Bauschlicher, Professor Ihsan Boustani, and Professor Kai-Ming Ho for sending us their optimized geometries of boron and silicon clusters. We are grateful to Professor George C. Schatz for much useful discussion on the transport theory, rotational sudden approximation, and evaluation of cross sections for rotating objects. We acknowledge Tamer Shoeib for his help with some of the calculations. This research has been supported by the Natural Sciences and Engineering Research Council of Canada and the Canadian Foundation for Innovation.

References and Notes

(1) Hill, H. H., Jr.; Siems, W. F.; St. Louis, R. H.; McMinn, D. G. *Anal. Chem.* **1990**, *62*, 1201A.
(2) von Helden, G.; Hsu, M. T.; Kemper, P. R.; Bowers, M. T. *J. Chem. Phys.* **1991**, *95*, 3835.
(3) von Helden, G.; Hsu, M. T.; Gotts, N. G.; Bowers, M. T. *J. Phys. Chem.* **1993**, *97*, 8182.
(4) Jarrold, M. F.; Constant, V. A. *Phys. Rev. Lett.* **1991**, *67*, 2994.
(5) von Helden, G.; Wyttenbach, T.; Bowers, M. T. *Science* **1995**, *267*, 1483.
(6) Clemmer, D. E.; Hudgins, R. R.; Jarrold, M. F. *J. Am. Chem. Soc.* **1995**, *117*, 10141.
(7) Dugourd, Ph.; Hudgins, R. R.; Clemmer, D. E.; Jarrold, M. F. *Rev. Sci. Instrum.* **1997**, *68*, 1122.
(8) Valentine, S. J.; Anderson, J.; Ellington, A. E.; Clemmer, D. E. *J. Phys. Chem. B* **1997**, *101*, 3891.
(9) Wu, C.; Siems, W. F.; Asbury, R. G.; Hill, H. H. *Anal. Chem.* **1998**, *70*, 4929.
(10) Buryakov, I.; Krylov, E.; Nazarov, E.; Rasulev, U. *Int. J. Mass Spectrom. Ion Processes* **1993**, *128*, 143.
(11) Purves, R. W.; Guevremont, R.; Day, S.; Pipich, C. W.; Matyjaszszyk, M. S. *Rev. Sci. Instrum.* **1998**, *69*, 4094.
(12) Hoaglund, C. S.; Valentine, S. J.; Clemmer, D. E. *Anal. Chem.* **1997**, *69*, 4156.
(13) Hoaglund, C. S.; Valentine, S. J.; Sporleder, C. R.; Reilly, J. P.; Clemmer, D. E. *Anal. Chem.* **1998**, *70*, 2236.
(14) Henderson, S. C.; Valentine, S. J.; Counterman, A. E.; Clemmer, D. E. *Anal. Chem.* **1999**, *71*, 291.
(15) Mason, E. A.; McDaniel, E. W. *Transport Properties of Ions in Gases*; Wiley: New York, 1988.
(16) Mack, E., Jr. *J. Am. Chem. Soc.* **1925**, *47*, 2468.
(17) Shvartsburg, A. A.; Jarrold, M. F. *Chem. Phys. Lett.* **1996**, *261*, 86.
(18) Mesleh, M. F.; Hunter, J. M.; Shvartsburg, A. A.; Schatz, G. C.; Jarrold, M. F. *J. Phys. Chem.* **1996**, *100*, 16082.
(19) Shvartsburg, A. A.; Schatz, G. C.; Jarrold, M. F. *J. Chem. Phys.* **1998**, *108*, 2416.
(20) Shvartsburg, A. A.; Liu, B.; Jarrold, M. F.; Ho, K. M. *J. Chem. Phys.* **2000**, *112*, 4517.
(21) Shvartsburg, A. A.; Liu, B.; Siu, K. W. M.; Ho, K. M. *J. Phys. Chem. A* **2000**, *104*, 6152.

(22) Liu, B.; Lu, Z. Y.; Pan, B. C.; Wang, C. Z.; Ho, K. M.; Shvartsburg, A. A.; Jarrold, M. F. *J. Chem. Phys*. **1998**, *109*, 9401.
(23) Shvartsburg, A. A.; Hudgins, R. R.; Dugourd, Ph.; Jarrold, M. F. *J. Phys. Chem. A* **1997**, *101*, 1684.
(24) Shvartsburg, A. A.; Hudgins, R. R.; Gutierrez, R.; Jungnickel, G.; Frauenheim, T.; Jackson, K. A.; Jarrold, M. F. *J. Phys. Chem. A* **1999**, *103*, 5275.
(25) Wyttenbach, T.; von Helden, G.; Bowers, M. T. *J. Am. Chem. Soc*. **1996**, *118*, 8355.
(26) Present analysis of the effect of thermal rotation on ionic mobilities in heavy buffer gases is within the confines of eq 1. In reality, the Rayleigh limit would be violated when $m_B \ll m$ does not hold and higher-order collision integrals become material (Hirschfelder, J. O.; Curtiss, C. F.; Bird, R. B. *Molecular Theory of Gases and Liquids*; Wiley: New York, 1964). These integrals ($\Omega_{avg}^{(1,2)}$, $\Omega_{avg}^{(1,3)}$, $\Omega_{avg}^{(2,2)}$, etc.) are presumably also affected by ionic rotation but in a way that probably differs from that for $\Omega_{avg}^{(1,1)}$ considered here.
(27) Ricca, A.; Bauschlicher, C. W., Jr. *Chem. Phys*. **1996**, *208*, 233.
(28) Boustani, I. *Int. J. Quantum Chem*. **1994**, *52*, 1081.
(29) Boustani, I. *Phys. Rev. B* **1997**, *55*, 16426.
(30) Lee, S.; Gotts, N. G.; von Helden, G.; Bowers, M. T. *Science* **1995**, *267*, 999.
(31) Lee, S.; Gotts, N.; von Helden, G.; Bowers, M. T. *J. Phys. Chem. A* **1997**, *101*, 2096.
(32) von Helden, G.; Porter, E.; Gotts, N. G.; Bowers, M. T. *J. Phys. Chem*. **1995**, *99*, 7707.
(33) Krishnamurthy, M.; de Gouw, J. A.; Bierbaum, V. M.; Leone, S. R. *J. Phys. Chem*. **1996**, *100*, 14908.
(34) de Gouw, J. A.; Krishnamurthy, M.; Bierbaum, V. M.; Leone, S. R. *Int. J. Mass Spectrom. Ion Processes* **1997**, *167/168*, 281.
(35) Rata, I.; Shvartsburg, A. A.; Horoi, M.; Frauenheim, Th.; Siu, K. W. M.; Jackson, K. A. *Phys. Rev. Lett*. **2000**, *85*, 546.
(36) Shvartsburg, A. A.; Liu, B.; Lu, Z. Y.; Wang, C. Z.; Jarrold, M. F.; Ho, K. M. *Phys. Rev. Lett*. **1999**, *83*, 2167.
(37) Shvartsburg, A. A.; Jarrold, M. F. *Phys. Rev. A: At., Mol., Opt. Phys*. **1999**, *60*, 1235.
(38) Shvartsburg, A. A.; Jarrold, M. F. *Chem. Phys. Lett*. **2000**, *317*, 615.
(39) Counterman, A. E.; Valentine, S. J.; Srebalus, C. A.; Henderson, S. C.; Hoaglund, C. S.; Clemmer, D. E. *J. Am. Soc. Mass Spectrom*. **1998**, *9*, 743.
(40) Valentine, S. J.; Counterman, A. E.; Hoaglund, C. S.; Reilly, J. P.; Clemmer, D. E. *J. Am. Soc. Mass Spectrom*. **1998**, *9*, 1213.
(41) Mao, Y.; Ratner, M. A.; Jarrold, M. F. *J. Phys. Chem. B* **1999**, *103*, 10017.
(42) Hudgins, R. R.; Jarrold, M. F. *J. Am. Chem. Soc*. **1999**, *121*, 3494.
(43) Wu, C.; Siems, W. F.; Klasmeier, J.; Hill, H. H. *Anal. Chem*. **2000**, *72*, 391.
(44) Wu, C.; Siems, W. F.; Hill, H. H. *Anal. Chem*. **2000**, *72*, 396.
(45) Karpas, Z.; Berant, Z. *J. Phys. Chem*. **1989**, *93*, 3021.
(46) Ring, S.; Naaman, R.; Rudich, Y. *Anal. Chem*. **1999**, *71*, 648.
(47) Shvartsburg, A. A.; Pederson, L. A.; Hudgins, R. R.; Schatz, G. C.; Jarrold, M. F. *J. Phys. Chem. A* **1998**, *102*, 7919.
(48) Shvartsburg, A. A.; Hudgins, R. R.; Dugourd, Ph.; Gutierrez, R.; Frauenheim, Th.; Jarrold, M. F. *Phys. Rev. Lett*. **2000,** *84*, 2421.